Precipitation phenomena in MC-Ni-Co cermet systems

EUN SIK KIM, SHINHOO KANG
School of Materials Science and Engineering, Seoul National University, Seoul 151-742, South Korea
E-mail: shinkang@plaza.snu.ac.kr

Ti(CN)-Ni-Co, WC-Ni-Co, and TaC-Ni-Co cermets were prepared, in order to understand the effect of carbide dissolution during the heating and sintering stages of the precipitation phenomena. Magnetic properties, such as magnetic saturation ($4\pi\sigma$) and coercive force (H_c), were measured and related to the observed changes in the microstructure. There is evidence in the TaC-Ni-Co system that early precipitation occurs during the heating stage. But they do not influence the final microstructure. Most of the dissolved carbides tend to re-precipitate on the growing particles during sintering while the remaining solutes in the melt precipitate in the binder during cooling, thus affecting the coercive force of cermets. The TEM analysis identified the precipitates as TiNi(TiCo), Ti(CN) in the Ti(CN)-Ni-Co cermet, Co_3W, WC in the WC-Ni-Co cermet, and Co_2Ta, TaC in the TaC-Ni-Co cermet.
© *2001 Kluwer Academic Publishers*

1. Introduction

In recent years TiC or Ti(CN)-based cermets have been the subject of considerable cutting tool materials [1–3]. TiC cermets are known to exhibit a higher degree of hardness and superior chemical stability at high temperatures. However, their low toughness prevents the complete replacement of WC the major carbide tool material with those materials. This led to research for the cermet tool material to the optimization of mechanical properties through the partial replacement of WC and the addition of other carbides and nitrides [4–6]. This issue of how to improve tool performance in cutting operations is a complex issue to explain. However, in many cases the tool industries have attempted to tailor the mechanical properties of cermets of known compositions by controlling the precipitation phenomena in the binder phase. To date, however, not many studies have been done in the area of precipitation phenomena in the binder region [7, 8].

The measurement of magnetic properties, such as magnetic saturation ($4\pi\sigma$) and coercive force (H_c), is a non-destructive method which is used by the tool industries to study the precipitation in the binder phase [7, 9–13]. Coercive force (H_c) is known to be a microstructure-sensitive property while magnetic saturation ($4\pi\sigma$) is not. The factors that most affect H_c are the size and number of precipitates. Thus, the measurement of H_c provides an insight into changes in microstructure. On the other hand the measurement of $4\pi\sigma$ can provide information about the composition of the binder phase. Since Ni and Co show ferromagnetic behavior in a magnetic field, the $4\pi\sigma$ value of a cermet is a function of volume percent of non-ferromagnetic phases [14, 15]. However, the size of carbide particles is known to have no effect on the $4\pi\sigma$ [16, 17].

It has been reported from WC-Co systems that the magnetic saturation ($4\pi\sigma$) of Co decreases linearly as W enters the binder phase. Naturally it increases when the precipitation of W from the solid solution occurs in the form of WC, Co_3W or Co_3W_3C. The precipitation of WC increases the $4\pi\sigma$ value more effectively than that of Co_3W or Co_3W_3C due to the conservation of Co in the binder. Roebuck *et al.* [13, 18] reported that the content of W in the binder phase can be quantitatively determined by measurements of the magnetic moment using the following relationship;

$$4\pi(\sigma_b + am_s)W_b = 4\pi\sigma_h \qquad (1)$$

where σ_b represents the magnetic moment of pure Co ($\sim$161 gauss cm^3/g), a is the derivative of magnetic saturation with respect to solute contents, m_s is the weight fraction of W dissolved in Co, and W_b the weight fraction of binder phase, respectively. The value of $4\pi\sigma_h$ is the magnetic saturation of the specimen. When W is dissolved, the corresponding value of a is -0.275 [18].

The coercive force (H_c) measures the level of resistance caused by the domain walls during the removal of magnetic field. Thus, the H_c is strongly dependent on the number and size of precipitates that cause a pinning effect. The largest value of H_c is known to occur when the diameter of the precipitate is equal to the domain wall width in Co ($\sim$200 Å). The undersized and oversized precipitates have only a negligible effect on the value of H_c. The H_c is calculated on the basis of pinning theory using the approach described by Gaunt [19].

$$H_c = H_0 \left(1 - \frac{25kT}{A\Delta\gamma} \right) \qquad (2)$$

	Particle size (μm)	Manufacturer
Ti($C_{0.5}N_{0.5}$)	3–5	Kennametal
WC	1.88	H.C.Starck
TaC	0.8–1.0	H.C.Starck
Co	1.63	Novamet
Ni	1.7	Novamet

where H_0 is the zero-temperature coercive force, k the Boltzmann constant, T the temperature, A the free area of wall, and $\Delta\gamma$ the energy barrier.

In this study Ti(CN)-Ni-Co, WC-Ni-Co, and TaC-Ni-Co systems were prepared in order to understand the effect of carbide dissolution during heating and sintering on the precipitation phenomena. The selected carbides represent the most common cermet materials for tool production. This study was designed to provide basic information for the understanding of precipitation in multi-component carbide systems such as Ti(CN)-WC-TaC-Ni-Co.

2. Experimental

The average size and manufacturers of the powders used in this experiment are shown in Table I. The compositions are fixed at Ti(CN)-, WC-, and TaC-15%Ni-15%Co (in mol. %). The powders were mixed and ball-milled in acetone for 12 hr using WC-Co balls and then compacted at a pressure of 50 MPa to produce a disk 10 mm in diameter. Specimens were heated in vacuum (5×10^{-4} torr) to various temperatures (1200–1600°C) and then cooled immediately. The heating rate was 10°C/min from room temperature to 1200°C and 3°C/min from 1200°C to 1600°C.

The coercive force (H_c) and magnetic saturation ($4\pi\sigma$) was measured with a Sigmameter, manufactured in Germany. The reported values in this study are the averages of 4 measurements. The magnetic saturation ($4\pi\sigma$) of a pure binder metal (50%Ni-50%Co) is 137 gauss cm^3/g. Transmission electron microscopy was done using a Philips CM30, Netherlands, for the analysis of the phases formed in the binder phase. The specimens for TEM observations were heated to 1500°C and cooled immediately. The composition of binder phase was also analyzed with EDS (energy dispersive spectroscopy).

3. Results and discussion
3.1. Effect of carbide dissolution in heating stage

In order to investigate the effect of carbide dissolution in the heating stage on the precipitation, the samples were heated to a designated temperature (1200–1600°C) and cooled immediately. The heating schedule of the samples is shown in Fig. 1. The eutectic temperature of the Co-C(Ni-C) system is 1320°C(1328°C) at 2.6(9) wt. % C. It is also known that liquid Ni starts to appear around 1350°C in the Ti(CN)-Ni system [20]. Thus, the dissociation and subsequent solid-state diffusion of carbides to the binder represent the dominant processes up to 1200°C. At higher temperatures ($\geq$1350°C) carbide
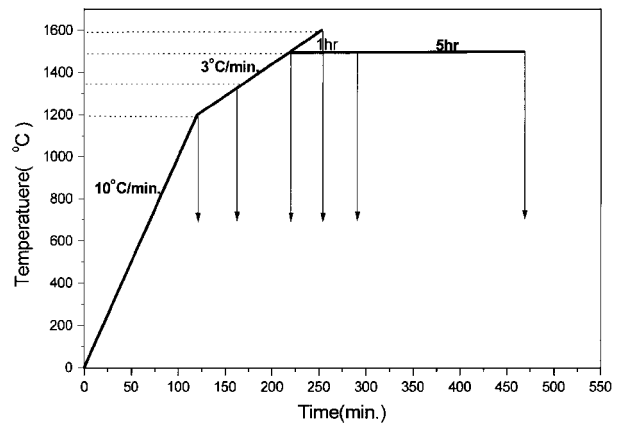

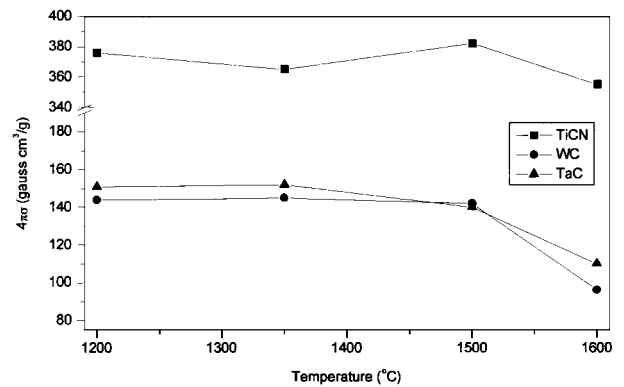*Figure 1* Heating schedules for the samples.

Figure 2 Measurements of $4\pi\sigma$ in Ti(CN)-Ni/Co, WC-Ni/Co, and TaC-Ni/Co systems sintered at 1200°C, 1350°C, 1500°C, and 1600°C.
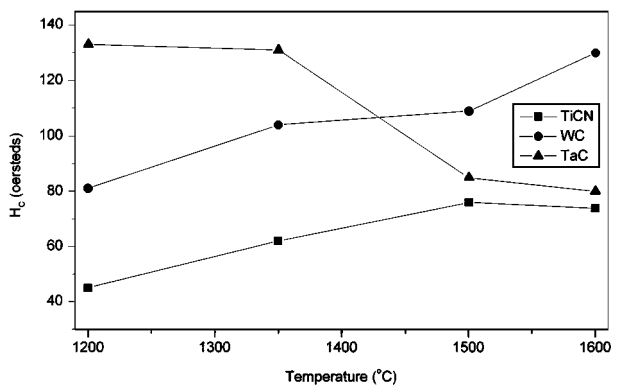

Figure 3 Measurements of H_C in Ti(CN)-Ni/Co, WC-Ni/Co, and TaC-Ni/Co systems sintered at 1200°C, 1350°C, 1500°C, and 1600°C.

dissolution becomes active and determines the solute content in the binder phase. The changes in the magnetic saturation ($4\pi\sigma$) and coercive force are plotted in Figs 2 and 3, respectively with respect to the final heating temperatures.

The magnetic saturation is expected to decrease rapidly with an increase in temperature due to a high solute content. However, all systems shown in Fig. 2 do not show this tendency until it reaches 1500°C. That is, an increase in the temperature does not always greatly change the final amount of solutes and precipitates in the binder. Based on the results at 1200°C in Figs 2 and 3, a noticeable precipitation in solid state occurred. The fluctuation in $4\pi\sigma$ in the Ti(CN)-Ni-Co system between 1350°C and 1500°C is unusual since the Ti(CN)

TABLE II Compositions of specimens (in m/o(w/o))

	Ti(CN)	WC	TaC	Ni	Co
A	70 (70.7)	-	-	15 (14.6)	15 (14.7)
B	-	70 (88.6)	-	15 (5.65)	15 (5.75)
C	-	-	70 (88.5)	15 (5.77)	15 (5.78)

phase has been reported to be extremely stable compared with WC and TaC. However, it may be regarded as a minor change. The values observed from Ti(CN)-Ni-Co are ∼2.5 times higher than they should be due to the high content of Ni and Co (Table II).

The values of $4\pi\sigma$ decrease in the temperature range of 1500°C–1600°C. The binder phase contains more non-ferromagnetic phase for the samples which have been exposed to temperatures above 1500°C. The largest reduction in magnetic saturation ($\sim$50 gauss cm^3/g) is found from the WC-Ni-Co system which has a relatively larger solubility limit than those of other systems. The reduction in $4\pi\sigma$ for the Ti(CN)-Ni-Co system is in the range of ∼30 gauss cm^3/g. Considering the sensitivity factor mentioned above, this is equivalent to ∼10 gauss cm^3/g at the same condition. The order of the reduction level is normally determined by the relative stability of the carbides.

When the solute becomes saturated during the sintering process, a continuous dissolution of carbides will cause re-precipitation on the surface of the carbides. Some of the solutes that remain in the binder begin to precipitate during cooling. These precipitates are mainly responsible for the coercive force of the cermets. The factors, such as microvoids, inclusions, and binder thickness also affect coercive force. However, it is generally accepted that the major factor in the change of H_c is the second phase. The contribution from other factors to H_c is assumed to be approximately the same in different sintering conditions.

The coercive force (H_c) of different cermets is shown in Fig. 3 with respect to the temperature. The coercive force (H_c) becomes stronger in the WC system as temperature increases, especially above 1500°C. The WC system reached the highest value at 1500°C and 1600°C. More fine precipitates tend to form in this system with an increase in the dissolution of WC between 1500 and 1600°C. In the case of the Ti(CN) system the H_c value is generally low in all conditions. The low dissolution tendency of Ti(CN) was further slowed by its large particle size. The enhanced dissolution of Ti(CN) at 1600°C did not result in a change in H_c.

In contrast, a high coercive force at 1350°C and a rapid drop at 1500°C were noted in the TaC-Ni-Co system. It would be an unusual phenomenon if normal precipitation occurred. This high H_c at 1200 and 1350°C could be related to the incomplete phase transformation from ε-Co to α-Co and to the formation of Co$_2$Ta during heating. Most of the dissolved TaC between 1350 and 1500°C seems to re-precipitate on the initial TaC particles, resulting in a low level of coercive force. During the cooling stage the saturated solutes precipitate within the binder phase again as TaC and Co$_2$Ta. The result obtained at 1600°C shows that further dissolution of TaC to the binder does not alter the precipitation dur-
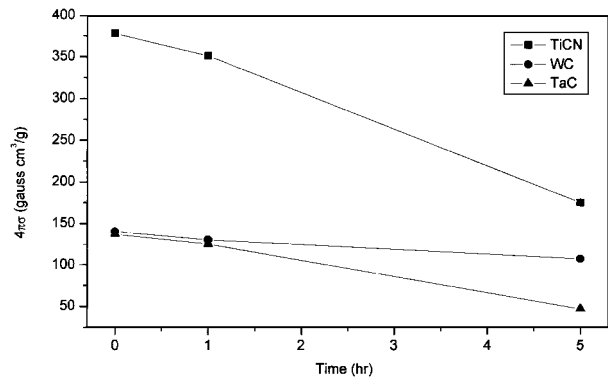

Figure 4 Measurements of $4\pi\sigma$ in Ti(CN)-Ni/Co, WC-Ni/Co, and TaC-Ni/Co systems sintered at 1500°C for 0 h, 1 h, and 5 h.
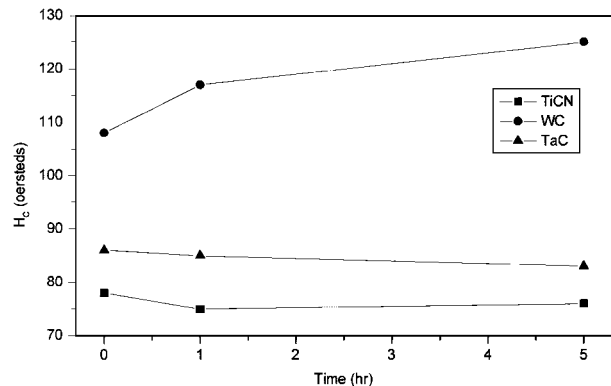

Figure 5 Measurements of H_C in Ti(CN)-Ni/Co, WC-Ni/Co, and TaC-Ni/Co systems sintered at 1500°C for 0 h, 1 h, and 5 h.

ing the cooling and simply coarsens the existing TaC in the binder, as shown with the Ti(CN) system.

3.2. Effect of sintering duration

Figs 4 and 5 show the effect of sintering time on magnetic saturation ($4\pi\sigma$) and coercive force (H_c) at 1500°C. When the sintering time gets longer, the level of magnetic saturation becomes lower. This tendency is due to the reduction of ferromagnetic substances by the formation of non-ferromagnetic precipitates or solid solutions. In the systems of study, TiNi, TiCo, Co$_3$W, Co$_3$W$_3$C, WC, and Co$_2$Ta are considered as the possible precipitates. The reduction rates, i.e., the slopes of the curves, of the saturation values, are about the same throughout the sintering time in all systems.

The WC-Ni-Co system exhibited no further increase in solute content or the amount of non-ferromagnetic materials in the binder with increasing sintering time. However, the Ti(CN) and TaC systems showed a continuous reduction in the magnetic saturation. The WC phase that has the lowest stability among the carbides of this study dissolves in the binder and appears to reach the saturation of solute within an hour at 1500°C. In contrast, the other two carbides appear to dissolve continuously with time. In Fig. 4, the Ti(CN) and TaC systems were found to have nearly the same reduction rate when the content of binder phase is taken into consideration.

The effect of sintering time on H_c is negligible, as shown in Fig. 5, compared to that on magnetic saturation at 1500°C. This would be expected to have

407

little change in H_c from the WC-Ni-Co system, which showed almost no change in magnetic saturation. Similarly, the H_c values of the Ti(CN) and TaC systems were expected to increase due to the increase in the non-ferromagnetic phases. Such phenomena were not observed. The reduction in the magnetic saturation of the TaC systems could be explained better by the increase in the solute content in the form of a solid solution since the solubility limit of Ta in Ni/Co at room temperature is 20 wt. %. However, the Ti(CN) system cannot be explained by solubility limits (<5 wt %). Rather, it can be explained by the coarsening of Co- or Ni-containing non-ferromagnetic precipitates such as TiCo and TiNi. The increased amount of coarsened precipitates will not enhance the coercive force.

According to Table I, the TaC particle has the smallest average size. The size of carbide particles is closely related to the amount of dissolved solutes. If all carbides have the same dissolution tendency, the TaC system would have the largest amount of dissolved carbides in a given time interval, because of the large surface area of the particles. However, the overall results indicate that the quantity of the dissolved carbide does not determine the magnetic properties of the cermets, i.e., precipitation phenomena.

3.3. The analysis of microstructure in the binder phase

Figs 6 through 8 show TEM micrographs of the binder phases, along with selected area diffraction (SAD) patterns of Ti(CN)-Ni-Co, WC-Ni-Co, and TaC-Ni-Co, respectively. The TEM specimens were prepared from samples which had been sintered at 1500°C for 0 hour. It is relatively simple to observe the structure, since each system contains 30 mol. % of binder phase. EDS analyses were also performed in order to identify the precipitates and the amount of solutes in the binder phase. Table III is the summary of the analysis.

As shown in the table, the contents of W, Ta, and Ti in the binder amount to 17.7, 5.1 and 1.9 wt. % respectively. These quantities include the contributions from precipitates and solutes present in a solid solution. The precipitates from the dissolved carbides could be

TABLE III Compositional analysis of various systems in the binder phase by EDS

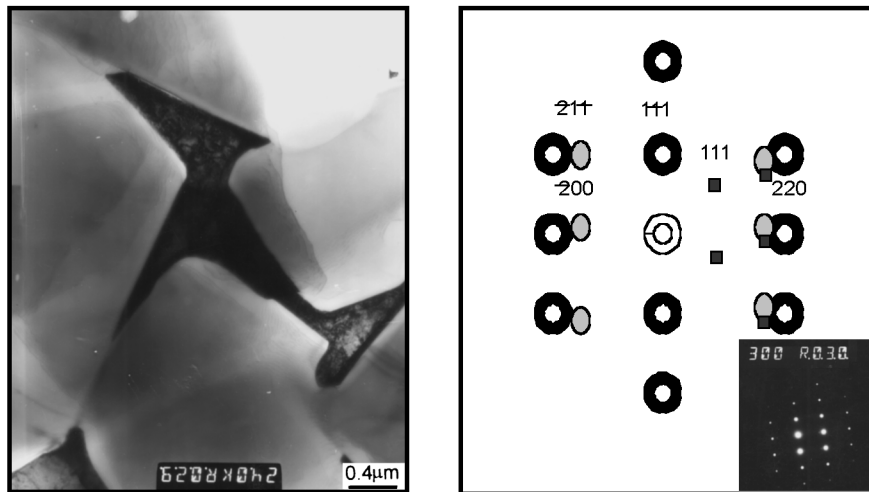| Systems (w/o)	Ni	Co	Others
Ti(CN)-Ni-Co	49.6	48.5	1.9Ti
TaC-Ni-Co	46.6	48.3	5.1Ta
WC-Ni-Co	43.5	38.8	17.7W

Figure 6 Transmission electron micrograph and phase analysis in Ti(CN)-Ni/Co system sintered at 1500°C for 0 h. Zone axes of matrix (⬤), Ti(CN) (■), and TiCo(TiNi) (⦿) are $[1\bar{1}2]$, $[1\bar{1}0]$, and $[022]$ respectively.
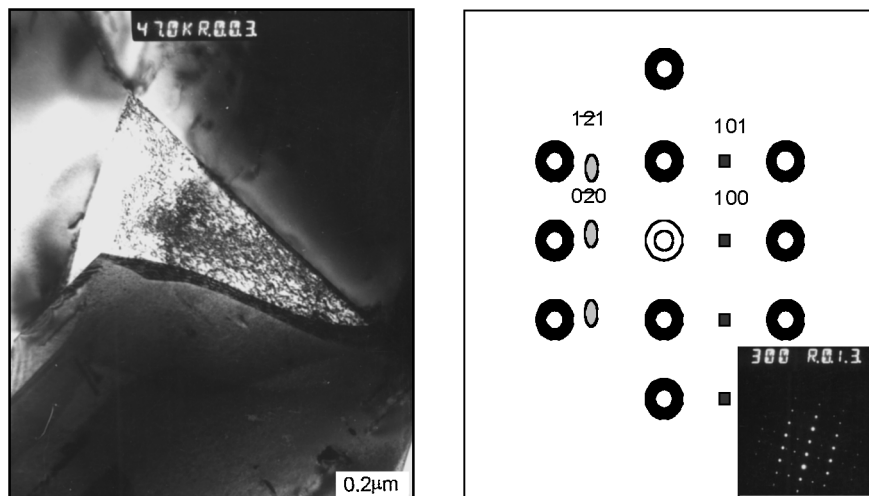

Figure 7 Transmission electron micrograph and phase analysis in WC-Ni/Co system sintered at 1500°C for 0 h. Zone axes of WC (⦿) and Co$_3$W (■) are $[0\bar{1}0]$ and $[10\bar{1}]$ respectively.
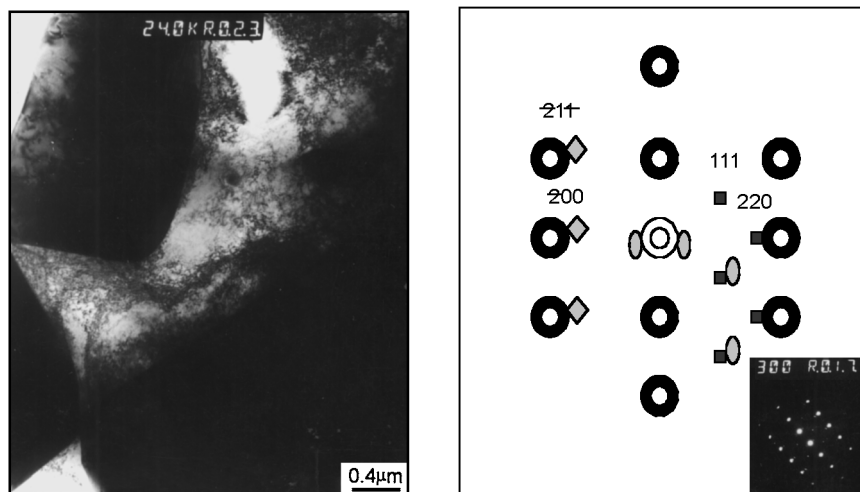
408

Figure 8 Transmission electron micrograph and phase analysis in TaC-Ni/Co system sintered at 1500°C for 0 h. Zone axes of Co_2Ta (◇) and TaC (■) are [011] and [1$\bar{1}$0] respectively. ⊙ is from double diffraction.

small, since the solubility limits of W, Ta and Ti are 15.1, 10, and 2.5 wt. % at room temperature, respectively. They could remain in the Ni/Co (1 : 1) binder in the form of solid solution at 25°C. There was little loss in the Ni and Co contents with the Ti(CN) and TaC systems. On the other hand, the amount of Co was shown to be more than that of Ni, by ∼5 wt.%, in the WC system. The reason for this has not yet been identified.

The binder phase is α(Co, Ni) solid solution according to the results of SAD in Figs 6–8. The diffraction pattern with zone axis of [1, −1, −2] in Fig. 6 is from the binder phase of the Ti(CN)-Ni-Co. It includes a small amount of Ti(CN) and TiCo (or TiNi) with their zone axes, [1, −1, 0] and [0, 1, 1], respectively. Among the various precipitates such as Ti_2Co, TiCo, $TiCo_2$, and $TiCo_3$, the TiCo phase that is the most stable up to 1325°C was dominant. The melting points of Ti_2Co, $TiCo_2$, and $TiCo_3$, are 1058, 1235, and 1200°C, respectively. It is possible for this system to have produced precipitates such as $TiCo_2$, and $TiCo_3$ due to limited diffusivity. All these phases appear to have dissolved with the appearance of the liquid phase. The formation of Ti(CN) in the binder is the result of the reduced mobility and limited solubility of the elements involved.

The diffraction pattern of the binder phase in WC-Ni-Co is shown in Fig. 7, and it shows the existence of the WC phase of the hcp structure as well as the Co_3W precipitates. Their zone axes are [0, −1, 0] and [1, 0, −1], respectively. Based on the result of compositional analysis (Table III) it can be reconfirmed that the dissolution of the WC phase is easier in Ni/Co liquid than other carbides. Possible phases, which could form in the system, are Co_3W, Co_3W_3C, and Co_7W_6. It is interesting to note that the Co_3W phase forms preferentially over Co_7W_6, which has greater high-temperature stability than Co_3W. The high solubility limit of W in the Ni/Co seemed to cause such a result. The melting points of Co_3W and Co_7W_6 are 1093 and 1689°C, respectively. The WC-Ni-Co system contains the largest volume of precipitates according to the result of H_c in Fig. 5. It is shown that H_c increases due to the presence of WC and Co_3W precipitates and to their low tendency toward coarsening.

The precipitates in the binder phase of TaC-Ni-Co system are TaC and Co_2Ta. Their zone axes are found to be [1, −1, 0] and [0, 1, 1], respectively from an analysis of the diffraction pattern in Fig. 8. In the Ta-Co binary phase diagram the Co_2Ta phase is the only compound formed. Based on its melting point (1593°C) it is relatively stable compared to other phases formed in different systems. Again, the formation of TaC is the result of the limited solubility and diffusivity of Ta and C at low temperatures.

4. Summary and conclusions
The magnetic properties of Ti(CN)-Ni-Co, TaC-Ni-Co, and WC-Ni-Co were measured in order to better understand the precipitation phenomena. The results from this experiment are summarized as below:

1. In all cases the dissolved carbides during the heating stage (1350–1500°C) were found to re-precipitate on the growing particles. The largest reduction in magnetic saturation ($4\pi\sigma$) was observed from the WC-Ni-Co system between 1500–1600°C and were found to be associated with the formation of WC and Co_3W. In general, the Ti(CN) system is slow to dissolve and precipitate among the various carbides due to its high stability and larger particle size. The unusual precipitation phenomena of the TaC-Ni-Co system (1350–1500°C) might be attributed to the dissolution of Co_2Ta and/or the retained ε-Co solid solution. Further, dissolved TaC between 1500–1600°C remained in the solid solution without adding to the number of fine precipitates.

2. The study of sintering time at 1500°C indicates that WC dissolves faster than other carbides, reaching saturation within an hour. On the other hand a continuous dissolution was found from the Ti(CN) and TaC systems without resultant precipitates. Most of the dissolved carbides re-precipitate on the remaining particles during sintering without affecting the coercive force of the cermets. The remaining solutes in the melt precipitate in the binder during cooling.

3. The precipitates in the binder of the systems are identified as Ti(CN), TiCo (or TiNi), TaC, Co_2Ta, WC, and Co_3W from the TEM diffraction analysis. These

phases are too fine to be visible from the binder regions by conventional TEM.

References

1. H. PASTOR, *Mat. Sci. and Eng.* **A105/106** (1988) 401.
2. P. ETTMAYER, H. KOLASKA, W. LENGAUER and K. DREYWER, *Int. J. Refract. Met. Hard Mat.* **13** (1995) 343.
3. F. QI and S. KANG, *Mat. Sci. and Eng.* **A251** (1998) 276.
4. S. KANG, *ibid.* **A209** (1996) 306.
5. H. JONSSON and B. ARONSSON, *J. of the Institute of Metals* **97** (1969) 281.
6. M. SHWARZKOPF, H. E. EWNER, H. F. FISCHMEISTER and W. SCHINTLMEISTER, *Mat. Sci. and Eng.* **A105/106** (1988) 225.
7. P. WALTER and H. GREWE, *Pow. Met. Inter.* **3** (1971) 88.
8. D. L. TILLWICK and I. JOFFE, *Appl. Phys.* **6** (1973) 1585.
9. L. J. DIJKSTRA and C. WERT, *Physical Review* **79** (1950) 979.
10. D. L. TILLWICK and I. JOFFE, *Scripta Metall.* **7** (1973) 479.
11. A. RAMESH, M. R. GOVINDARAJU, D. C. JILES and S. B. BINER, *IEEE Trans. on Magn.* **32** (1966) 4836.
12. E. W. LEE and J. E. L. BISHOP, *Proc. Phys. Soc.* **89** (1966) 661.
13. B. ROEBUCK, *Int. J. of Refrac. Metals and Hard Mat.* **14** (1996) 419.
14. V. A. TRACEY, *Refrac. Metals and Hard Mat.* **11** (1992) 137.
15. J. HINNUBER and O. RUDIGER, *Cobalt* **19** (1963) 57.
16. H. JONSSON, *Pow. Metall.* **15** (1972) 1.
17. H. SUZUKI, T. YAMAMOTO and K. HAYASHI, *Jap. Soc. of Pow. Meta.* **13** (1966) 42.
18. B. ROEBUCK and E. A. ALMOND, *Inter. Mat. Reviews* **33** (1988) 90.
19. P. GAUNT, *J. Appl. Phys.* **43** (1972) 637.
20. S. Y. AHN and S. KANG, unpublished work.